International Journal of Heat and Mass Transfer 70 (2014) 378–388

Contents lists available at ScienceDirect

International Journal of Heat and Mass Transfer

journal homepage: www.elsevier.com/locate/ijhmt

Influence of ambient temperature on heat transfer in the human eye during exposure to electromagnetic fields at 900 MHz

Teerapot Wessapan [a], Phadungsak Rattanadecho [b,*]

[a] School of Aviation, Eastern Asia University, Pathumthani 12110, Thailand
[b] Center of Excellence in Electromagnetic Energy Utilization in Engineering (CEEE), Department of Mechanical Engineering, Faculty of Engineering, Thammasat University (Rangsit Campus), Pathumthani 12120, Thailand

ARTICLE INFO

Article history:
Received 5 July 2013
Received in revised form 4 November 2013
Accepted 4 November 2013

Keywords:
Electromagnetic fields
Temperature distribution
Specific absorption rate
Human eye
Heat transfer

ABSTRACT

The topic of temperature increase in human tissue when exposed to EM fields, particularly those radiated to the eye, has been of interest for many years. This study presents a numerical analysis of the specific absorption rate (SAR) and the heat transfer in a heterogeneous two-dimensional human eye model exposed to TM-mode of electromagnetic (EM) fields of 900 MHz at various power densities. In this study, the effects of ambient temperature and power density on the temperature distributions and fluid flow in the eye during exposure to electromagnetic fields were systematically investigated. The electric field, SAR, temperature distribution and fluid flow in various tissues in the eye during exposure to EM fields were obtained by numerical simulation of EM wave propagation and a heat transfer model. The heat transfer model was then developed based on the porous media theories. The study highlights heat transfer and fluid flow in the eye during exposure to EM fields at different ambient temperatures. This study indicated that when the eye exposed to EM fields at the frequency of 900 MHz, the highest electric field intensity and SAR values at the chosen frequency was in the cornea. At the highest power density of 100 mW/cm^2, the absorbed EM energy is converted to heat causes a further increase of 3 °C in corneal temperature in cases of hot, moderate and cold ambient temperatures. The result shows important information related to a complex interaction between ambient temperature, fluid flow and temperature distribution in the eye during exposure to electromagnetic fields. Moreover, this study also showed that the power density had a strong influence on the temperature increase and fluid flow in the eye.

1. Introduction

The human eye temperature increase is important for both laboratory and clinical investigations [1–3]. Environmental conditions, namely ambient temperature and EM fields influence the temperature increase in the eye. It is known that the eye is one of the most sensitive organs to environmental factors such as electromagnetic (EM) fields and extreme temperature conditions. This is due to the fact that the crystalline lens and the cornea are non-vascular tissue with low metabolism, and the eye has no thermal sensors and protective reflexes. In recent years, there has been increasing public concern with the interaction between the eye and the EM fields. Most previous studies of the temperature increase in the eye caused by EM fields mainly focused on the effect of heat generated from volumetric heating by EM absorption without concerning in regards to the ambient temperatures external. Most of them have not been accounted for the different ambient temperature situations during exposure to EM fields causing unrealistic results. Therefore, the inclusion of different ambient temperatures to the simulation is needed to completely explain the actual process of interaction between the EM fields and the eye in the realistic situation. Numerical analysis of the heat transfer and fluid flow in the eye exposed to EM fields has provided useful information on absorption of EM energy for the eye under a variety of exposure conditions.

In the past, there have been reports on the effects of EM fields on the eye [4,5]. Nevertheless, the analysis generally was conducted based on the maximum SAR values permitted by public safety standards [6,7]. The research on transport phenomena in a porous medium subject to EM fields is sparse except for our group. Some researcher investigated the effects of EM fields on the eye temperature [8]. However, most previous studies of human exposed to EM fields hardly considered the heat transfer causing an incomplete analysis to the results. The thermal modeling of human tissue is important as a tool to investigate the effect of external heat sources and to predict the abnormalities in the tissue. At the beginning, most studies of heat transfer analysis in the eye used heat conduction equation [9–15]. Some studies carried out

* Corresponding author. Tel.: +66 2564 3001 9; fax: +66 2564 3010.
E-mail addresses: teerapot@yahoo.com (T. Wessapan), ratphadu@engr.tu.ac.th (P. Rattanadecho).

0017-9310/$ - see front matter © 2013 Elsevier Ltd. All rights reserved.
http://dx.doi.org/10.1016/j.ijheatmasstransfer.2013.11.009

Nomenclature

C	specific heat capacity (J/(kg K))
E	electric field intensity (V/m)
e	tear evaporation heat loss (W/m^2)
f	frequency of incident wave (Hz)
H	magnetic field (A/m)
h	convection coefficient (W/m^2 K)
j	current density (A/m^2)
k	thermal conductivity (W/(m K))
n	normal vector
p	pressure (N/m^2)
Q	heat source (W/m^3)
T	temperature (K)
u	velocity (m/s)
t	time

Greek letters

B	volume expansion coefficient (1/K)
μ	magnetic permeability (H/m)
ε	permittivity (F/m)
σ	electric conductivity (S/m)
ω	angular frequency (rad/s)
ρ	density (kg/m^3)
ω_b	blood perfusion rate (1/s)
Γ	external surface area

Subscripts

am	ambient
b	blood
ext	external
i	subdomain
met	metabolic
r	relative
ref	reference
0	free space, initial condition

on the natural convection in the eye based on heat conduction model [20,21]. Ooi and Ng [21,22] studied the effect of aqueous humor (AH) hydrodynamics on the heat transfer in the eye based on heat conduction model. Meanwhile, the bioheat equation, introduced by Pennes [23,24] based on the heat diffusion equation for a blood perfused tissue, is used for modeling of the heat transfer in the eye as well [25,26]. Ooi and Ng also developed a three-dimensional model of the eye [27], extending their two-dimensional model [26]. They also state that the use of a two-dimensional model may be promising in simulating the heat transfer phenomena inside the human eye with a single set of parameters and symmetric boundary conditions. Recently, porous media models have been utilized to investigate the transport phenomena in biological media instead of a simplified bioheat model [28–30]. Shafahi and Vafai [31] proposed the porous media along with a natural convection model to analyze the eye thermal characteristics during exposure to thermal disturbances. The other research groups have been tried to conduct the numerical analysis of heat and EM dissipation in the eye [11–19]. Ooi et al. have been tried to conduct the advanced model using the coupled model of heat and laser irradiation in the eye [32]. Results from a similar model of Ooi et al. [32] for various applications were also presented in continuation [33–36].

Our research group has tried to numerically investigate the temperature increase in the human tissue subjected to EM fields in many problems [37–45]. Wessapan et al. [37,38] utilized a 2D finite element method to obtain the SAR and temperature increase in the human body exposed to leakage EM waves. Wessapan et al. [39,40] developed a three-dimensional human head model in order to investigate the SAR and temperature distributions in human head during exposure to the mobile phone radiation. Keangin et al. [41–43] carried out on the numerical simulation of the liver cancer treated using the complete mathematical model considered the coupled model of EM wave propagation, heat transfer and mechanical deformation in the biological tissue in the couple's way. Wessapan et al. [44,45] investigated the SAR and temperature distributions in the eye during exposed to EM waves at 900 and 1800 MHz using the porous media theory.

Although the advance modeling of the eye using porous media and natural convection theory have been used in the various heat transfer problems [20,21,31], most studies of the human eye exposed to the EM fields have not been considered the different ambient temperatures to the simulations. There are few studies on the temperature and EM field interaction in a realistic physical model of the human organs especially the eye that concerning the existence of the hotness and coldness of the ambient air due to the complexity of the problem, even though it is also influential to the heat transfer. Therefore, in order to provide information on the levels of exposure and health effects from the EM field exposure adequately, it is essential to consider the ambient temperature in an analysis.

This study presents the simulation of the SAR and temperature distributions in an anatomical human eye exposed to EM fields at various power densities. In this study, the effects of ambient temperature and power density on the temperature distributions and fluid flow in the eye during exposure to electromagnetic fields were systematically investigated. The electric field, SAR and the temperature distribution in various tissues in the eye during exposure to EM fields were obtained by numerical simulation of EM wave propagation and a heat transfer model. The heat transfer model was then developed based on the porous media theories. The work described in this paper is substantially extended from our previous work [44] by further enhancing the focus on the effect of ambient temperature. In this study, a two-dimensional heterogeneous human eye model was used to simulate the SAR, temperature distributions and fluid flow in the eye model. The EM wave propagation in the eye was investigated by using Maxwell's equations. An analysis of the heat transfer in the eye exposed to TM-mode of EM fields at 900 MHz was investigated using a developed heat transfer model (based on porous media theory) which was firstly proposed by Shafahi and Vafai [31]. In the heterogeneous eye model, the effects of ambient temperature and power density on the temperature distribution and fluid flow in the eye are systematically investigated. The electric field, SAR, temperature distribution and fluid flow are obtained by numerical simulation of the EM wave propagation and heat transfer equations based on porous media theory, are presented. Actually, corneal surface temperature changes rapidly when blinking. However, in this work, the model excluded the presence of eyelid and blinking effect as well as the metabolic heat generation in order to ease the modeling procedures. The obtained values represent the accurate phenomena to determine the temperature increase and fluid flow in the eye as well as indicate the limitations that must be considered as the temperature increase due to EM energy absorption from EM field exposure at different ambient temperatures.

2. Formulation of the problem

The human eye is exposed daily to radiation from sources such as mobile phones, and other EM fields commonly found in our daily life. Fig. 1 shows the eye subjected to EM radiation at various ambient conditions. These EM fields radiate into the eye that causes heating in the deeper tissue, which leads to tissue damage and cataract formation [2]. Due to ethical consideration, exposing the human to EM fields for experimental purposes is limited. It is more convenient to develop a realistic human eye model through the numerical simulation. A highlight of this work is the illustration of the transport phenomena, including the heat transfer and fluid flow in the eye during exposure to EM fields at different ambient temperatures. The analyses of the SAR and the heat transfer in the eye exposed to EM fields will be illustrated in Section 3. The system of governing equations as well as the boundary conditions is solved numerically using the finite element method (FEM) via COMSOL^{TM} Multiphysics.

3. Methods and model

When the EM waves propagate from one medium to another, they can be absorbed, reflected, refracted, or transmitted, depending on the dielectric property of the material and the operating frequency of the EM source. The first step in evaluating the effects of a certain exposure to EM fields in the eye is to determine the induced internal EM fields and its spatial distribution. Thereafter, EM energy absorption which results in temperature increase in the eye and other interactions will be able to be considered.

3.1. Physical model

In this study, the two-dimensional model of the eye, which follows the physical model in the previous research [31], is developed. Fig. 2 shows the two-dimensional eye model used in this study. This model comprises seven types of tissue including cornea, anterior chamber, posterior chamber, iris, sclera, lens and vitreous. These tissues have different dielectric and thermal properties. The choroid and sclera layers are relatively thin compared to the sclera. To simplify the problem, these layers are modeled as part of the sclera. The iris and sclera, which have the same properties, are modeled together as one homogenous region [21]. The dielectric and thermal properties of tissue are given in Tables 1 and 2, respectively. Each tissue is assumed to be homogeneous and electrically as well as thermally isotropic.

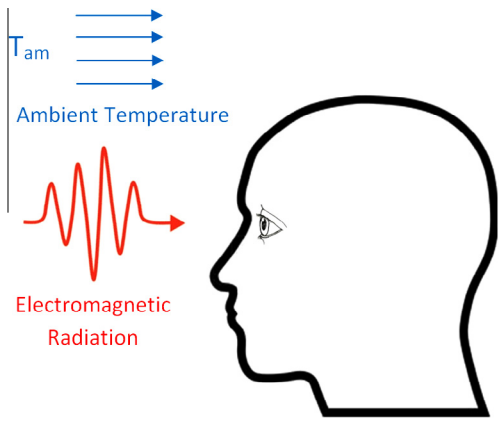

Fig. 1. Human eye subjected to EM radiation at various ambient temperatures.

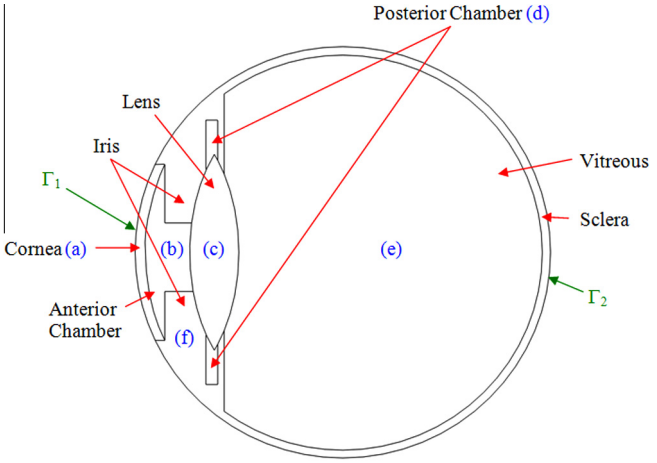

Fig. 2. Human eye vertical cross section [31].

Table 1
Dielectric properties of tissues at 900 MHz and 1800 MHz [46,47].

Tissue	Frequency: 900 MHz	
	ε_r	σ (S/m)
Cornea *(a)*	52.0	1.85
Anterior chamber *(b)*	73.0	1.97
Lens *(c)*	51.3	0.89
Posterior chamber *(d)*	73.0	1.97
Vitreous *(e)*	74.3	1.97
Sclera *(f)*	52.1	1.22
Iris *(f)*	52.1	1.22

3.2. Equations for EM wave propagation analysis

The mathematical models are developed to predict the electric fields and the SAR with respect to the temperature gradient in the eye. To simplify the problem, the following assumptions are made:

1. The EM wave propagation is modeled in two dimensions.
2. The eye in which the EM waves interact proceeds in the open region.
3. The free space is truncated by scattering boundary condition.
4. The model assumes that dielectric properties of each tissue are constant.
5. In the eye, the EM waves are characterized by transverse magnetic fields (TM-mode).

The EM wave propagation in the eye is calculated using Maxwell's equations which mathematically describe the interdependence of the EM waves. The general form of Maxwell's equations is simplified to demonstrate the EM fields penetrated in the eye as the following equation:

$$\nabla \times \left(\left(\varepsilon_r - \frac{j\sigma}{\omega \varepsilon_0} \right)^{-1} \nabla \times H_z \right) - \mu_r k_0^2 H_z = 0 \tag{1}$$

where H is the magnetic field (A/m), μ_r is the relative magnetic permeability, ε_r is the relative dielectric constant, $\varepsilon_0 = 8.8542 \times 10^{-12}$ F/m is the permittivity of free space, k_0 is the free space wave number (m^{-1}).

3.2.1. Boundary condition for wave propagation analysis

EM energy is emitted by an EM radiation device and falls on the eye with a particular power density. Therefore, boundary condition

Table 2
Thermal properties of the eye [21].

Tissue	ρ (kg/m^3)	k (W/m °C)	C_p (J/kg °C)	μ (N s/m^2)	β (1/K)
Cornea *(a)*	1050	0.58	4178	–	–
Anterior chamber *(b)*	996	0.58	3997	0.00074	0.000337
Lens *(c)*	1000	0.4	3000	–	–
Posterior chamber *(d)*	996	0.58	3997	–	–
Vitreous *(e)*	1100	0.603	4178	–	–
Sclera *(f)*	1050	1.0042	3180	–	–
Iris *(f)*	1050	1.0042	3180	–	–

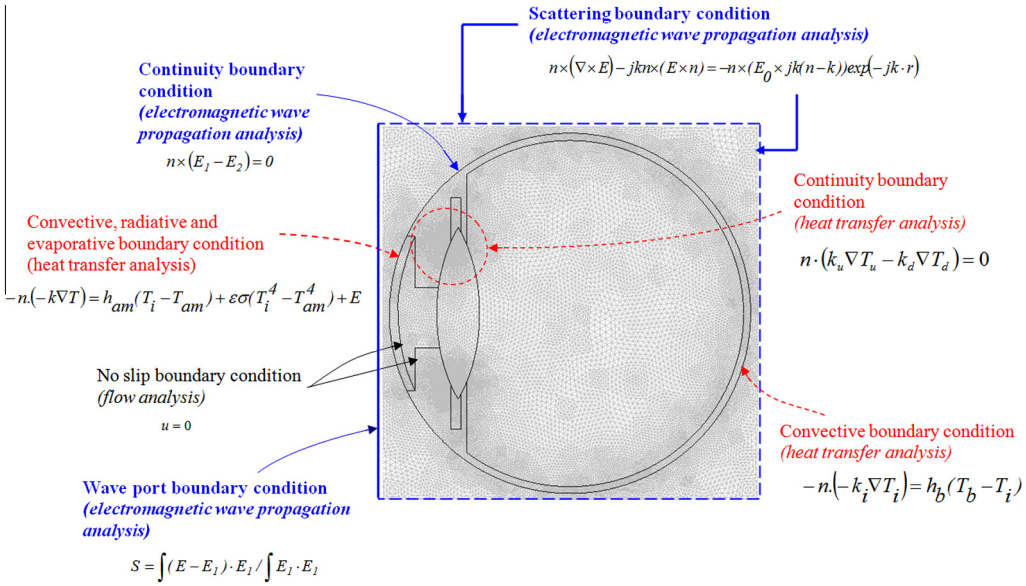

Fig. 3. Boundary condition for analysis of EM wave propagation and heat transfer.

for solving EM wave propagation, as shown in Fig. 3, is described as follows:

It is assumed that the uniform wave flux falls on the left side of the eye. Therefore, at the left boundary of the considered domain, an EM simulator employs TM wave propagation port with specified power density,

$$S=\int((E-E_1)\cdot E_1)dA_1\Big/\int(E_1\cdot E_1)dA_1 \tag{2}$$

where E is the electric field intensity (V/m), and E_1 is fundamental value of electric field for port 1.

Boundary conditions along the interfaces between different mediums, for example, between air and tissue or tissue and tissue, are considered as continuity boundary condition,

$$n\times(E_1-E_2)=0 \tag{3}$$

The outer sides of the calculated domain, i.e., free space, are considered as scattering boundary condition [37],

$$n\times(\nabla\times E_z)-jkE_z=-jk(1-k\cdot n)E_{0z}\exp(-jk\cdot r) \tag{4}$$

where k is the wave number (m^{-1}), σ is the electrical conductivity (S/m), n is the normal vector, $j=\sqrt{-1}$, and E_0 is the incident plane wave (V/m), E_z is the transverse component of the electric field.

3.3. Interaction of EM fields and human tissues

Interaction of EM fields with biological tissue can be defined in the term of the SAR. When the EM waves propagate through the tissue, the energy of EM waves is absorbed by the tissue. The SAR is defined as power dissipation rate normalized by material density [37]. The SAR is given by,

$$SAR=\frac{\sigma}{\rho}|E|^2 \tag{5}$$

where σ is the electric conductivity (S/m), and ρ is the tissue density (kg/m^3).

3.4. Equations for heat transfer and flow analysis

To solve the thermal problem, the coupled model of the EM wave propagation and unsteady heat transfer as well as the boundary conditions is investigated. The temperature distribution is corresponded to the SAR. This is because the SAR in the eye distributes owing to energy absorption. Thereafter, the absorbed energy is converted to thermal energy, which increases the tissue temperature.

Heat transfer analysis of the eye is modeled in two dimensions. To simplify the problem, the following assumptions are made:

1. The human tissue is a bio-material with constant thermal properties.
2. There is no phase change of substance in the tissue.
3. There is a local thermal equilibrium between the blood and the tissue.
4. There is no chemical reaction in the tissue.
5. The thermoregulation mechanism has been neglected

For the flow analysis, the following assumptions on the flow of aqueous humor are made:

1. The aqueous humor is modeled as an incompressible Newtonian fluid,
2. Buoyancy effects are modeled by the Boussinesq approximation.

This study utilized the pertinent thermal model based on the porous media theory [31] to investigate the heat transfer behavior of the eye when exposed to the EM fields.

In this study, the motion of fluid is considered only inside the anterior chamber [21]. There is a blood flow in the iris/sclera part, which plays a role to adjust the eye temperature with the rest of the body [31]. For the rest parts, the metabolic heat generation is neglected based on the fact that these comprise mainly water [21]. The equation governing the flow of heat in cornea, posterior chamber, lens and vitreous are resembled the classical heat conduction equation given in Eq. (6).

$$\rho_i C_i \frac{\partial T_i}{\partial t} = \nabla \cdot (k_i \nabla T_i) + Q_{ext}; \quad i = a, c, d, e \tag{6}$$

where T is the tissue temperature (K), ρ is the tissue density (kg/m^3) and C is the heat capacity of tissue (J/kg K).

This model accounts for the existence of AH in the anterior chamber. The heat transfer process consists of both the conduction and natural convections, which can be written as follows:

Continuity equation:

$$\nabla \cdot u_i = 0; \quad i = b \tag{7}$$

Momentum equation:

$$\rho_i \frac{\partial u_i}{\partial t} + \rho_i u_i \nabla \cdot u_i = -\nabla p_i + \nabla \cdot [\mu(\nabla u_i + \nabla u_i^T)] + \rho_i g \beta_i (T_i - T_{ref}); \quad i = b \tag{8}$$

where i denotes each subdomain in the eye model as shown in Fig. 2, β is the volume expansion coefficient (1/K), u is the velocity (m/s), p is the pressure (N/m^2), μ is the dynamic viscosity of AH (N s/m^2), t is the time, and T_{ref} is the reference temperature considered here as 37 °C. The effects of buoyancy due to the temperature gradient are modeled using the Boussinesq approximation which states that the density of a given fluid changes slightly with temperature but negligibly with pressure [21].

Energy equation:

$$\rho_i C_i \frac{\partial T_i}{\partial t} - \nabla \cdot (k_i \nabla T_i) = -\rho C_i u_i \cdot \nabla T_i + Q_{ext}; \quad i = b \tag{9}$$

The sclera/iris is modeled as a porous medium with the blood perfusion, which assumes that local thermal equilibrium exits between the blood and the tissue. The blood perfusion rate used is 0.004 1/s. A modified Pennes' bioheat equation [21,28] is used to calculate the temperature distribution in the sclera/iris.

$$(1-\varepsilon)\rho_i C_i \frac{\partial T_i}{\partial t} = \nabla \cdot ((1-\varepsilon) k_i \nabla T_i) + \rho_b C_b \omega_b (T_b - T_i) + Q_{ext}; \quad i = f \tag{10}$$

where k is the thermal conductivity of tissue (W/m K), T_b is the temperature of blood (K), ρ_b is the density of blood (kg/m^3), C_b is the specific heat capacity of blood (J/kg K), ω_b is the blood perfusion rate (1/s), and Q_{ext} is the external heat source term (EM heat-source density) (W/m^3).

In the analysis, the porosity (ε) used is assumed to be 0.6. The heat conduction between the tissue and the blood flow is approximated by the blood perfusion term, $\rho_b C_b \omega_b (T_b - T)$.

The external heat source term is equal to the resistive heat generated by the EM fields (EM power absorbed), which defined as [37]

$$Q_{ext} = \frac{1}{2}\sigma_{tissue} |\bar{E}|^2 = \frac{\rho}{2} \cdot SAR \tag{11}$$

where σ_{tissue} is the electric conductivity of tissue (S/m).

3.4.1. Boundary condition for heat transfer analysis

The heat transfer analysis excluding the surrounding space is considered only in the eye. The cornea surface as shown in Fig. 3, is considered as the convective, radiative, and evaporative boundary conditions.

$$-n.(-k\nabla T) = h_{am}(T_i - T_{am}) + \varepsilon\sigma(T_i^4 - T_{am}^4) + e \quad \text{on } \Gamma_1 \quad i = a \tag{12}$$

where Γ_i is the external surface area corresponding to section i, e is the tear evaporation heat loss (W/m^2), T_{am} is the ambient temperature (K), h_{am} is the convection coefficient (W/m^2 K).

The temperature of blood generally assumed to be the same as the body core temperature causes heat to be transferred into the eye [21]. The surface of the sclera is assumed to be a convective boundary condition

$$-n \cdot (-k_i \nabla T_i) = h_b (T_b - T_i) \quad \text{on } \Gamma_2 \quad i = f \tag{13}$$

where h_b is the convection coefficient of blood (65 W/m^2 K).

3.4.2. Boundary condition for flow analysis

The internal surfaces of the anterior chamber as shown in Fig. 3, are specified with no slip condition for the momentum equations (Eq. (8))

$$u = 0 \tag{14}$$

3.5. Calculation procedure

In this study, the finite element method is used to analyze the transient problems. The computational scheme is to assemble finite element model and compute a local heat generation term by performing an EM calculation using tissue properties. In order to obtain a good approximation, a fine mesh is specified in the sensitive areas. This study provides a variable mesh method for solving the problem as shown in Fig. 4. The system of governing equations as well as the boundary conditions are then solved. All computational processes are implemented using COMSOL™ Multiphysics, to demonstrate the phenomenon that occurs in the eye exposed to the EM fields.

The 2D model is discretized using triangular elements and the Lagrange quadratic is then used to approximate the temperature and SAR variations across each element. The convergence test is carried out to identify the suitable number of elements required. The convergence curve resulting from the convergence test is

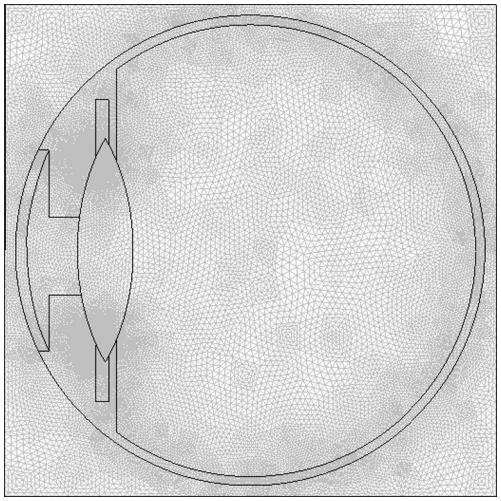

Fig. 4. A two-dimensional finite element mesh of the eye model.

shown in Fig. 5. This convergence test leads to the grid with approximately 10,000 elements. It is reasonable to assume that, at this element number, the accuracy of the simulation results is independent from the number of elements.

4. Results and discussion

In this analysis, the effects of ambient temperature and power density on the temperature distributions and fluid flow in the eye during exposure to electromagnetic fields were systematically investigated. The coupled model of the EM wave propagation and unsteady heat transfer as well as the boundary conditions is solved numerically. For the simulation, the dielectric and thermal properties are directly taken from Tables 1 and 2, respectively.

4.1. Verification of the model

In order to verify the accuracy of the present numerical models, the case without EM fields of the simulated results from this study are validated against the numerical results with the same geometric model obtained by Shafahi and Vafai [31]. Moreover, the numerical results are then compared to the experimental results of the rabbit obtained from Lagendijk [8]. The validation case assumes that the rabbit body temperature is 38.8 °C, the tear evaporation heat loss is 40 W/m^2, the ambient temperature is 25 °C, and the convection coefficient of ambient air is 20 W/m^2 K. The results of the selected test case are depicted in Fig. 6 for temperature distribution in the eye. Fig. 6 clearly shows a good agreement of the temperature distribution in the eye between the present solution and that of Shafahi and Vafai [31] and Lagendijk [9]. In the figure, the simulated results provides a good agreement with the simulated results obtained from Shafahi and Vafai [31]. This favorable comparison lends confidence in the accuracy of the present numerical model.

4.2. Electric field distribution

In this section, the effect of power density on electric field distribution in the eye is systematically investigated. To illustrate the penetrated electric field distribution inside the eye, the predicted results obtained from our proposed models are required. Fig. 7 shows the simulation of an electric field pattern inside the eye exposed to the EM fields in TM mode operating at the frequencies of 900 MHz propagating along the vertical cross section human eye model. Due to the different dielectric characteristics of the various tissue layers, a different fraction of the supplied EM energy will become absorbed in each layer in the eye. It can be seen that the higher values of electric fields at all power densities occur in the outer part area of the eye, especially in cornea, and lens. The electric fields deep inside the eye are extinguished where the electric fields attenuate due to the absorbed EM energy and are then converted to heat. Moreover, the electric field distribution also showed a strong dependence on the dielectric properties of the tissue. It is found that the maximum electric field intensity at the higher power density is greater than that of the lower power density. The maximum electric field intensities are 123.9, 277.0, and 391.8 V/m at the power densities of 10, 50, and 100 mW/cm^2, respectively. The three highest electric field intensity values in the human eye at all power densities occur in cornea, lens, and iris, respectively. This is because the lower value of their dielectric properties (ε_r) shown in Table 1 which corresponds to Eq. (1), as well as these tissues located close to the exposed surface, by which it causes the electromagnetic field can penetrate easily into these tissues.

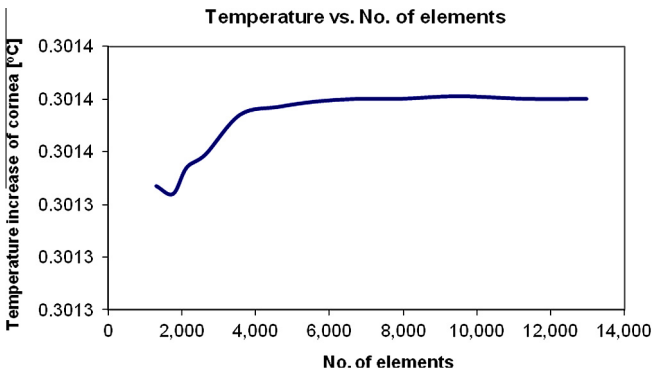

Fig. 5. Grid convergence curve of the 2D model.

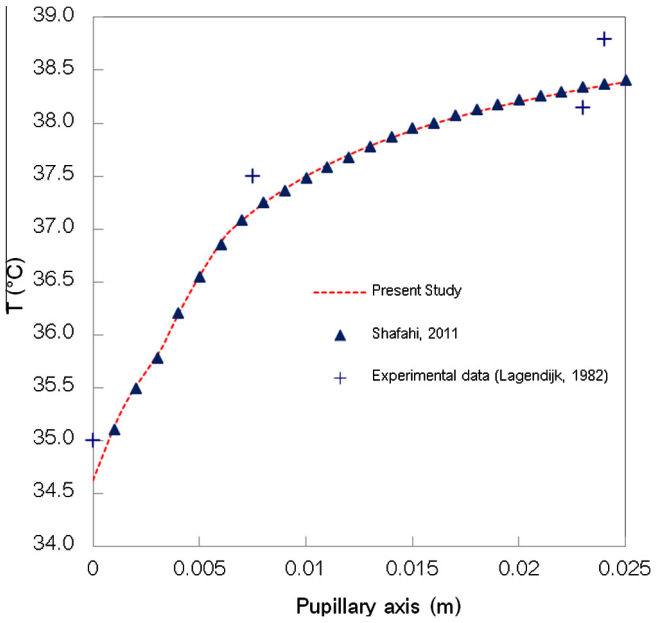

Fig. 6. Comparison of the calculated temperature distribution to the temperature distribution obtained by Shafahi and Vafai [31], and the Lagendijk's experimental data [9]; h_{am} = 20 W/m^2 K and T_{am} = 25 °C.

4.3. SAR distribution

SAR is a measure of the rate at which energy is absorbed by the eye when exposed to the electromagnetic fields. Fig. 8 shows the SAR distribution evaluated on the vertical cross section of the eye exposed to the EM frequencies of 900 MHz at the power densities of 10, 50, and 100 mW/cm^2. It is evident from the figure that the results of the SAR values in the eye (Fig. 8) are increased corresponding to the electric field intensities (Fig. 7). Besides the electric field intensity, the magnitude of the dielectric and thermal properties in each tissue will directly affect SAR values in the eye. For all power densities, the highest SAR values are obtained in the region of the corneal surface. This is because the cornea has a much higher value of its electrical conductivity (σ) than those of lens and iris. The second main reason is the position of the cornea located close to the exposed surface, at which the electric field intensity is strongest. It is found that the SAR distribution pattern in the eye, which corresponds to Eq. (5), is strongly dependent on the effect of the dielectric properties (σ, shown in Table 1) and thermal properties (ρ, shown in Table 2). The maximum SAR values are 13.5, 67.5, and 135.2 W/kg at the power densities of 10, 50, and 100 mW/cm^2, respectively.

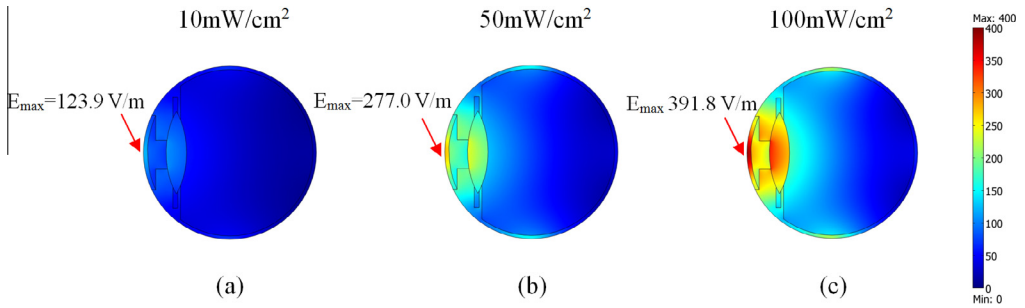

Fig. 7. Electric field distribution (V/m) in the eye exposed to the EM power densities of (a) 10 mW/cm^2 (b) 50 mW/cm^2 and (c) 100 mW/cm^2.

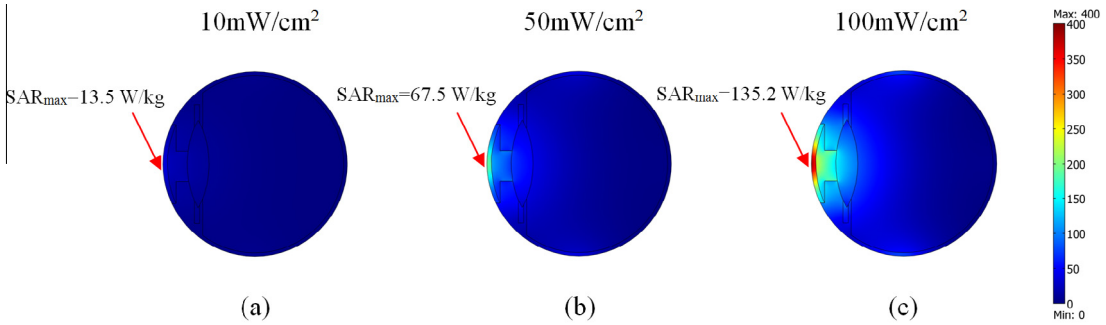

Fig. 8. SAR distribution (W/kg) in the eye exposed to the EM power densities of (a) 10 mW/cm^2 (b) 50 mW/cm^2 and (c) 100 mW/cm^2.

4.4. Temperature distribution

The following discussions focus on the transport phenomena that occur within the eye exposed to EM fields in hot, moderate and cold ambient temperatures. In this study, the effect of thermoregulation mechanisms has been neglected due to the small temperature increase occurred during exposure process. The convective coefficient due to the blood flow inside the sclera is set to 65 W/m^2 K [21]. In order to study the heat transfer in the eye, the coupled model of EM wave propagation and unsteady heat transfer as well as the boundary conditions is then investigated. Due to these coupled effects, the electric field distribution in Fig. 7 and the SAR distribution in Fig. 8 are then converted into heat by absorption of the tissue. Fig. 9 shows the temperature distribution in the eye exposed to the various EM power densities at the ambient temperature (T_{am}) of 50, 37, and 0 °C. The temperature in the eye (Fig. 9) is increased corresponding to the SAR (Fig. 8). This is because the electric fields in the eye attenuate owing to the energy absorbed and thereafter the absorbed energy is converted to thermal energy, which increases the eye temperature.

In case without EM fields, when the ambient temperature is higher than the eye temperature, namely 50 °C (shown in Fig. 9a), heat convected and radiated from the ambient air is flowing into the eye, and the eye temperature rises above normal body temperature. When the ambient temperature is close to the eye temperature, namely 37 °C (shown in Fig. 9b), heat does not transfer as readily via radiation, convection, and conduction pass through the ocular surface. In this case, the eye normally maintains the normal set body temperature at 37 °C. When the ambient temperature is lower than the eye temperature, namely 0 °C (shown in Fig. 9c), heat flows out of the eye and into the ambient air readily via convection and radiation, and the eye temperature cools down below a normal body temperature. In case without EM fields, the maximum temperatures inside the eye are 40.53, 37.0, and 36.41 °C for the ambient temperatures of 50, 37, and 0 °C, respectively.

In case of ambient temperature interaction with EM fields, the volumetric heating gives rise to an energy transfer into the eye being exposed to electromagnetic fields. In Fig. 9, the effect of power density (the power irradiated on the human eye surface) has also investigated. This figure shows the comparison of the temperature distribution within the eye at time approaching to steady state condition with the frequency of 900 MHz corresponding to the power densities of 10, 50, and 100 mW/cm^2. It is found that the power densities significantly influence the temperature increase within the eye. Greater power density provides greater heat generation inside the eye, thereby increasing the eye temperature. In the hot ambient temperature (T_{am} = 50 °C), the maximum temperatures in the eye are 40.82, 42.0, and 43.48 °C at the power densities of 10, 50, and 100 mW/cm^2, respectively. In the moderate ambient temperature (T_{am} = 37 °C), the maximum temperatures in the eye are 37.31, 38.53, and 40.06 °C at the power densities of 10, 50, and 100 mW/cm^2, respectively. In the cold ambient temperature (T_{am} = 0 °C), the maximum temperatures in the eye are 36.48, 36.77, and 37.24 °C at the power densities of 10, 50, and 100 mW/cm^2, respectively. At the maximum power density of 100 mW/cm^2, the temperature increased by 2.95, 3.06, and 0.83 °C for the ambient temperatures of 50, 37, and 0 °C, respectively.

Consider the temperature distribution at the extrusion line (Fig. 10). Fig. 11 shows the steady state temperature distribution versus pupillary axis (along the extrusion line) of the eye exposed and unexposed to the EM power density of 100 mW/cm^2 at various ambient temperatures. This figure shows that the effect of ambient temperature have a substantial impact on the temperature distribution in the eye for all cases.

In case of hot ambient temperatures (*with EM fields*) of 40, 50, and 60 °C (Fig. 11a), the heat generated by EM fields cannot be released into the ambient environment via radiation, convection, and conduction pass through the ocular surface, but in the opposite direction, heat from the ambient is flowing into the eye. In this case, heat dissipation by blood perfusion is therefore a major

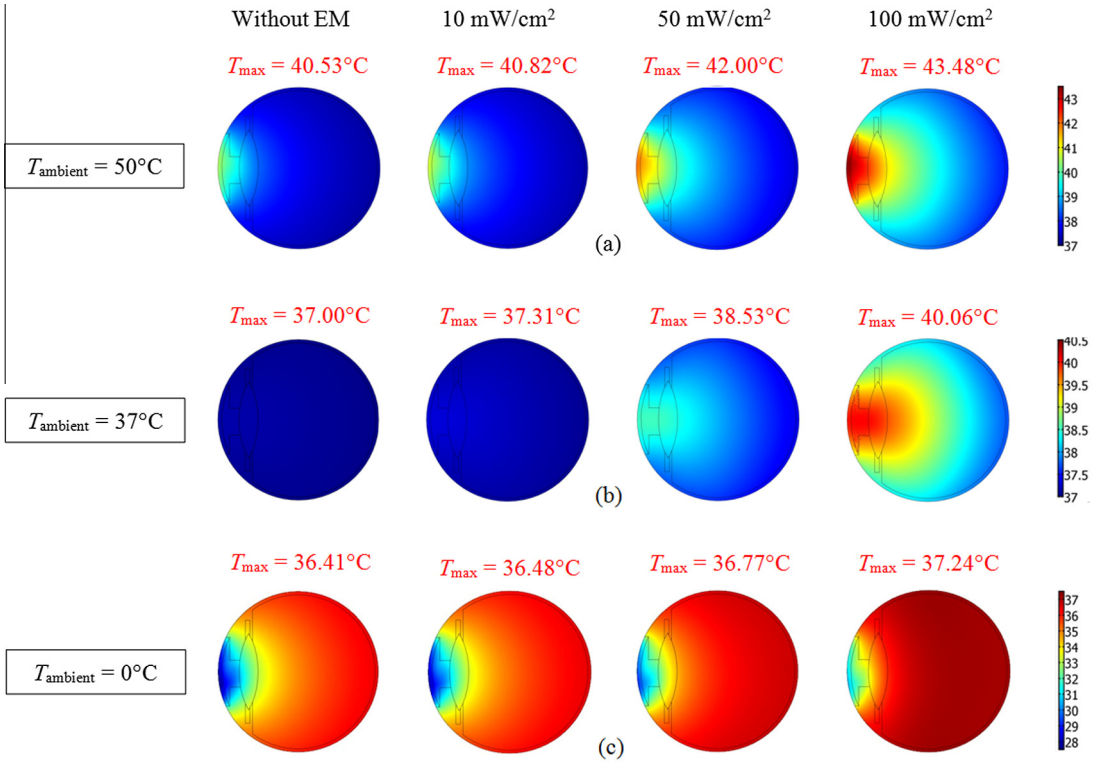

Fig. 9. The temperature distribution in the eye exposed to the various EM power densities at the ambient temperatures of (a) 50 °C (b) 37 °C and (c) 0 °C.

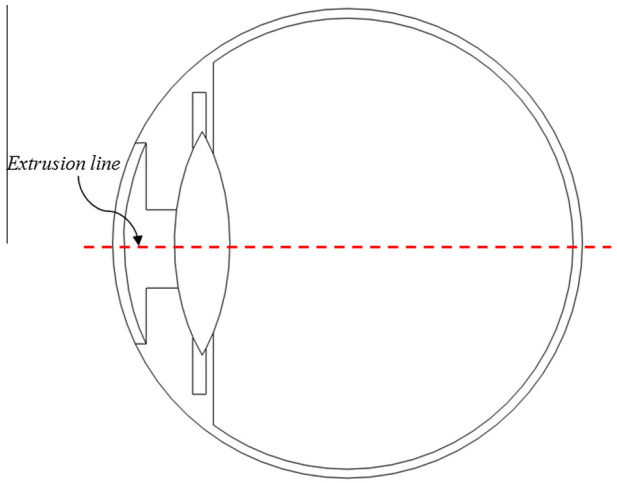

Fig. 10. The extrusion line in the eye where the temperature distribution is considered.

mechanism for reducing the eye temperature. The accumulated heat in combination of EM energy and ambient air raises the eye temperature up to 46 °C. This high temperature in the regions of cornea and lens may leads to damage eyesight and tissue destruction [2,3].

However, *in case of cold ambient temperatures* (*with EM fields*) of −10, 0, and 10 °C (Fig. 11b), the heat generated by EM fields flows out of the eye and into the ambient air much easier than that of the hot ambient temperature, and the eye temperature stays below the normal body temperature. In this case, the presence of blood perfusion provides buffer characteristic to the eye temperature, while the natural convection within the anterior chamber, shown in Fig. 12, plays important roles in enhancing the cooling process in the eye. It can be seen that for EM exposure at the cold ambient temperature is significantly safer than that of the hot ambient temperature. The temperature distribution patterns of all cases (−10, 0, and 10 °C) are nearly the same, which corresponds to the SAR patterns in Fig. 8.

Fig. 12 shows the circulatory patterns within the anterior chamber in the eye exposed to the EM power density of 100 mW/cm^2 at various ambient temperatures. These circulatory patterns within the anterior chamber do not only vary corresponding to the power densities, but also vary corresponding to that of the ambient temperature. *In case of hot ambient temperature* (50 °C) *both with and without EM fields,* a clockwise circulation thus appears in the anterior chamber, shown in Fig. 12a. This seemed to imply that the heat gradually travels inward passes through the front of the eye (cornea) to the lens. *In case of moderate ambient temperature* (37 °C) *with EM fields*, it is found that the natural convection and formation of two circulatory patterns with opposite direction in the anterior chamber, shown in Fig. 12b, play a role on the cooling processes in the eye, especially in the inner corneal surface. The circulation pattern implies that the generated heat in the anterior chamber is transferred in two directions; one is to the corneal surface, and the other to the lens surface. *In case of cold ambient temperature* (0 °C) *both with and without EM fields*, a counterclockwise circulation thus appears in the anterior chamber, shown in Fig. 12c. This seemed to imply that the direction of heat transfer travels outward from the lens surface. The circulation pattern in each case significantly different from each other, this is because each case exhibited a different heating pattern.

In comparison of cases with EM fields, in the case of *moderate ambient temperature*, the circulatory pattern has a lower speed, than that of the *hot and cold ambient temperature*. In the case with low flow speed, the heat transfer in the anterior chamber occurs mainly by conduction across the fluid layer. While in the case of *hot or cold ambient temperature* with higher flow speeds, different

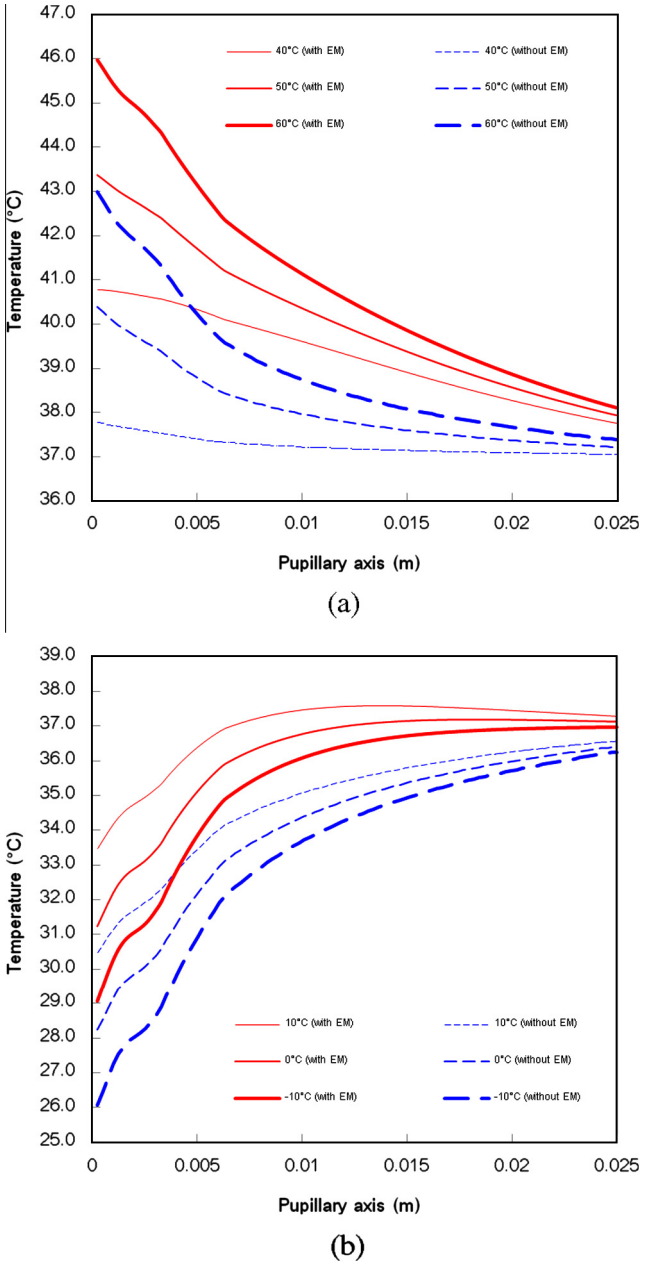

Fig. 11. Temperature distribution versus papillary axis of the eye exposed to the EM power density of 100 mW/cm^2 at (a) high ambient temperature and (b) low ambient temperature.

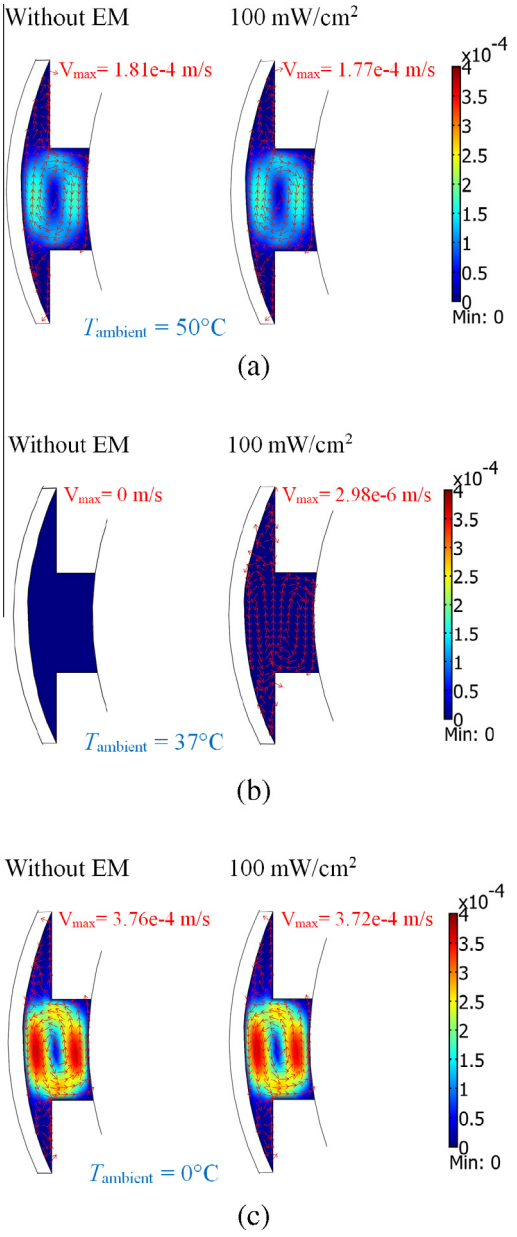

Fig. 12. The velocity distribution inside the anterior chamber non-exposed and exposed to the EM at the ambient temperatures of (a) 50 °C (b) 37 °C and (c) 0 °C.

flow regimes are encountered, with a progressively increasing heat transfer. In this case, convective heat transfer plays a significant role in transferring heat.

A comparison of circulatory patterns within the anterior chamber between the case with and without EM fields shows insignificant difference in the flow of *hot and cold ambient temperature* except in the case of *moderate ambient temperature*. This is because large temperature gradients produced by extreme ambient temperatures in the case of hot and cold ambient temperature causes the thermal boundary conditions play a more dominant role than volumetric heating by EM fields. Based on this study, it can be concluded that the flow patterns vary corresponding to the temperature gradient in the eye. Therefore, in a lower temperature gradient, the circulatory patterns have a lower speed, where a circulatory pattern with a higher temperature gradient flows faster.

In this study, the maximum temperature increase in the eye exposed to the EM fields with the power density of 100 mW/cm^2 at the ambient temperatures of 50, 37, and 0 °C are 2.95, 3.06, and 0.83 °C, respectively. It is found that as the ambient temperature increases, there is an increase in insensible to EM fields of the eye (unresponsiveness associated with EM energy absorb). This may cause potentially serious eye damage especially in case of ambient temperature that is higher than the normal body temperature.

5. Conclusions

In this study, the effects of ambient temperature and power density on the temperature distributions and fluid flow in the eye during exposure to electromagnetic fields were systematically investigated. The electric field, SAR and the temperature distribution in various tissues in the eye during exposure to EM fields were

obtained by numerical simulation of EM wave propagation and a heat transfer model was then developed based on the porous media theories.

It is found that the temperature distributions in the eye induced by the EM fields are related to the effect of the interaction among the dielectric properties, thermal properties, blood perfusion, and penetration depth of the EM power. Moreover, the increasing temperature of the eye has also been accompanied by an increase in extreme ambient conditions, not only directly to the specific energy absorbed (SAR). The result shows important information related to a complex interaction between ambient temperature, fluid flow and temperature distribution in the eye during exposure to electromagnetic fields. This study also showed that the power density had a strong influence on the temperature increase and fluid flow in the eye. At the highest power density of 100 mW/cm^2, the absorbed EM energy is converted to heat causes a further increase of 3 °C in corneal temperature in cases of hot, moderate and cold ambient temperatures. The obtained values represent the accurate phenomena to determine the temperature increase in the eye and indicate the limitations that must be considered as the temperature increase due to EM energy absorption from EM field exposure at different ambient temperatures.

Thus health effect assessment of the EM field exposure requires the utilization of the most accurate numerical simulation of the thermal model along with the SAR model. A study will also be developed to a more realistic 3D model for simulations and to study the temperature dependency of dielectric property in the future. This will allow a better understanding of the realistic situation of the interaction between the EM fields and the eye.

Acknowledgments

This work has been financially supported by the Thailand Research Fund (TRF), the Commission on Higher Education (CHE) and Eastern Asia University.

References

[1] R.D. Freeman, I. Fatt, Environmental influences on ocular temperature, Invest. Ophthalmol. 12 (8) (1973) 596–602.
[2] C. Buccella, V.D. Santis, M. Feliaiani, Prediction of temperature increase in human eyes due to RF sources, IEEE Trans. Electromagn. Compat. 49 (4) (2007) 825–833.
[3] J.C. Lin, Cataracts and cell-phone radiation, IEEE Trans. Electromagn. Compat. 45 (1) (2003) 171–174.
[4] O. Fujiwara, A. Kato, Computation of sar inside eyeball for 1.5-GHz microwave exposure using finite-difference time domain technique, IEICE Trans. E77-B (1994) 732–737.
[5] A. Karampatzakis, T. Samaras, Numerical modeling of heat transfer and fluid flow transfer in the human eye under millimeter wave exposure, Bioelectromagnetics 34 (2013) 291–299.
[6] International Commission on Non-Ionizing Radiation Protection (ICNIRP), Guidelines for limiting exposure to time-varying electric, magnetic and electromagnetic fields (up to 300 GHz), Health Phys. 74 (1998) 494–522.
[7] IEEE, IEEE Standard for Safety Levels with Respect to Human Exposure to Radio Frequency Electromagnetic Fields, 3 kHz to 300 GHz, 1999, IEEE Standard C95 1, 1999.
[8] A. Taflove, M.E. Brodwin, Computation of the electromagnetic fields and induced temperature within a model of the microwave-irradiated human eye, IEEE Trans. Microwave Theory Tech. 23 (11) (1975) 888–896.
[9] J.J.W. Lagendijk, A mathematical model to calculate temperature distribution in human and rabbit eye during hyperthermic treatment, Phys. Med. Biol. 27 (1982) 1301–1311.
[10] J. Scott, A finite element model of heat transport in the human eye, Phys. Med. Biol. 33 (1988) 227–241.
[11] J. Scott, The computation of temperature rises in the human eye induced by infrared radiation, Phys. Med. Biol. 33 (1988) 243–257.
[12] E.H. Amara, Numerical investigations on thermal effects of laser–ocular media interaction, Int. J. Heat Mass Transfer 38 (1995) 2479–2488.
[13] A. Hirata, S. Matsuyama, T. Shiozawa, Temperature rises in the human eye exposed to EM waves in the frequency range 0.6–6 GHz, IEEE Trans. Electromagn. Compat. 42 (4) (2000) 386–393.
[14] K.J. Chua, J.C. Ho, S.K. Chou, M.R. Islam, On the study of the temperature distribution within a human eye subjected to a laser source, Int. Commun. Heat Mass Transfer 32 (2005) 1057–1065.
[15] W. Limtrakarn, S. Reepolmaha, P. Dechaumphai, Transient temperature distribution on the corneal endothelium during ophthalmic phacoemulsification: a numerical simulation using the nodeless variable element, Asian Biomed. 4 (6) (2010) 885–892.
[16] E.Y.K. Ng, J.H. Tan, U.R. Acharya, J.S. Suri, Human Eye Imaging and Modeling, CRC Press, Florida, 2012, ISBN 978-1-4398-6993-2.
[17] D. Sumeet, U.R. Acharya, E.Y.K. Ng, Computational Analysis of Human Eye with Application, WSPC Press, Singapore, 2011, ISBN 978-981-4340-29-8.
[18] E.Y.K. Ng, U.R. Acharya, J.S. Suri, A. Campilho, Image Analysis and Modeling in Ophthalmology, CRC Press, Florida, 2014, ISBN 978-1-4665-5930-1.
[19] E.Y.K. Ng, U.R. Acharya, R.M. Rangayyan, J.S. Suri, Ophthalmology Imaging and Applications, Florida, 2014. ISBN: 978-1-4665-5913-4.
[20] S. Kumar, S. Acharya, R. Beuerman, A. Palkama, Numerical solution of ocular fluid dynamics in a rabbit eye: parametric effects, Ann. Biomed. Eng. 34 (2006) 530–544.
[21] E. Ooi, E.Y.K. Ng, Simulation of aqueous humor hydrodynamics in human eye heat transfer, Comput. Biol. Med. 38 (2008) 252–262.
[22] E.H. Ooi, E.Y.K. Ng, Effects of natural convection inside the anterior chamber, Int. J. Numer. Methods Biomed. Eng. 27 (2011) 408–423.
[23] H.H. Pennes, Analysis of tissue and arterial blood temperatures in the resting human forearm, J. Appl. Physiol. 1 (1948) 93–122.
[24] H.H. Pennes, Analysis of tissue and arterial blood temperatures in the resting human forearm, J. Appl. Physiol. 85 (1) (1998) 5–34.
[25] V.M.M. Flyckt, B.W. Raaymakers, J.J.W. Lagendijk, Modeling the impact of blood flow on the temperature distribution in the human eye and the orbit: fixed heat transfer coefficients versus the pennes bioheat model versus discrete blood vessels, Phys. Med. Biol. 51 (2006) 5007–5021.
[26] E.Y.K. Ng, E.H. Ooi, FEM simulation of the eye structure with bioheat analysis, Comput. Methods Programs Biomed. 82 (2006) 268–276.
[27] E.H. Ooi, E.Y.K. Ng, Ocular temperature distribution: a mathematical perspective, J. Mech. Med. Biol. 9 (2009) 199–227.
[28] A. Nakayama, F. Kuwahara, A general bioheat transfer model based on the theory of porous media, Int. J. Heat Mass Transfer 51 (2008) 3190–3199.
[29] S. Mahjoob, K. Vafai, Analytical characterization of heat transfer through biological media incorporating hyperthermia treatment, Int. J. Heat Mass Transfer 52 (2009) 1608–1618.
[30] K. Khanafer, K. Vafai, Synthesis of mathematical models representing bioheat transport, Adv. Numer. Heat Transfer 3 (2009) 1–28.
[31] M. Shafahi, K. Vafai, Human eye response to thermal disturbances, ASME J. Heat Transfer 133 (2011) 011009.
[32] E.H. Ooi, W.T. Ang, E.Y.K. Ng, A boundary element model of the human eye undergoing laser thermokeratoplasty, Comput. Biol. Med. 28 (2008) 727–738.
[33] E.H. Ooi, W.T. Ang, E.Y.K. Ng, A boundary element model for investigating the effects of eye tumor on the temperature distribution inside the human eye, Comput. Biol. Med. 28 (2009) 727–738.
[34] J.H. Tan, E.Y.K. Ng, U.R. Acharya, C. Chee, Study of normal ocular thermogram using textural parameters, Infrared Phys. Technol. 53 (2010) 120–126.
[35] J.H. Tan, E.Y.K. Ng, U.R. Acharya, Evaluation of tear evaporation from ocular surface by functional infrared thermography, Med. Phys. 37 (2010) 6022–6034.
[36] J.H. Tan, E.Y.K. Ng, U.R. Acharya, Evaluation of topographical variation in ocular surface temperature by functional infrared thermography, Infrared Phys. Technol. 54 (2011) 469–477.
[37] T. Wessapan, S. Srisawatdhisukul, P. Rattanadecho, Numerical analysis of specific absorption rate and heat transfer in the human body exposed to leakage electromagnetic field at 915 MHz and 2450 MHz, ASME J. Heat Transfer 133 (2011) 051101.
[38] T. Wessapan, S. Srisawatdhisukul, P. Rattanadecho, The effects of dielectric shield on specific absorption rate and heat transfer in the human body exposed to leakage microwave energy, Int. Commun. Heat Mass Transfer 38 (2011) 255–262.
[39] T. Wessapan, P. Rattanadecho, Numerical analysis of specific absorption rate and heat transfer in human head subjected to mobile phone radiation, ASME J. Heat Transfer 134 (2012) 121101.
[40] T. Wessapan, S. Srisawatdhisukul, P. Rattanadecho, Specific absorption rate and temperature distributions in human head subjected to mobile phone radiation at different frequencies, Int. J. Heat Mass Transfer 55 (2012) 347–359.
[41] P. Keangin, T. Wessapan, P. Rattanadecho, Analysis of heat transfer in deformed liver cancer modeling treated using a microwave coaxial antenna, Appl. Therm. Eng. 31 (16) (2011) 3243–3254.
[42] P. Keangin, T. Wessapan, P. Rattanadecho, An analysis of heat transfer in liver tissue during microwave ablation using single and double slot antenna, Int. Commun. Heat Mass Transfer 38 (2011) 757–766.
[43] P. Rattanadecho, P. Keangin, Numerical study of heat transfer and blood flow in two-layered porous liver tissue during microwave ablation process using single and double slot antenna, Int. J. Heat Mass Transfer 58 (2013) 457–470.
[44] T. Wessapan, P. Rattanadecho, Specific absorption rate and temperature increase in human eye subjected to electromagnetic fields at 900 MHz, ASME J. Heat Transfer 134 (2012) 091101.
[45] T. Wessapan, P. Rattanadecho, Specific absorption rate and temperature increase in the human eye due to electromagnetic fields exposure at different frequencies, Int. J. Heat Mass Transfer 64 (2013) 426–435.

[46] P. Bernardi, M. Cavagnaro, S. Pisa, E. Piuzzi, Specific absorption rate and temperature increases in the head of a cellular-phone user, IEEE Trans. Microwave Theory Tech. 48 (7) (2000) 1118–1126.

[47] S. Park, J. Jeong, Y. Lim, Temperature rise in the human head and brain for portable handsets at 900 and 1800 MHz, in: Proceedings of the Fourth International Conference on Microwave and Millimeter Wave Technology, vol. 1, 2004, pp. 966–969.